Applied Catalysis B: Environmental 165 (2015) 572–578

Contents lists available at ScienceDirect

Applied Catalysis B: Environmental

journal homepage: www.elsevier.com/locate/apcatb

Sulfate radicals induced from peroxymonosulfate by magnetic ferrospinel MFe_2O_4 (M = Co, Cu, Mn, and Zn) as heterogeneous catalysts in the water

Yueming Ren[a,*], Lingqiang Lin[a], Jun Ma[b,*], Jing Yang[a], Jing Feng[a], Zhuangjun Fan[a]

[a] Key Laboratory of Superlight Materials & Surface Technology, Ministry of Education, College of Material Science and Chemical Engineering, Harbin Engineering University, Harbin 150001, PR China
[b] State Key Laboratory of Urban Water Resource and Environment, Harbin Institute of Technology, Harbin 150090, PR China

ARTICLE INFO

Article history:
Received 5 June 2014
Received in revised form 17 October 2014
Accepted 20 October 2014
Available online 27 October 2014

Keywords:
Sulfate radical
Hydroxyl radical
Peroxymonosulfate
Spinel ferrite
DBP

ABSTRACT

Magnetic ferrospinel MFe_2O_4 (M = Co, Cu, Mn, and Zn) prepared in a sol–gel process was introduced as catalyst to generate powerful radicals from peroxymonosulfate (PMS) for refractory di-n-butyl phthalate (DBP) degradation in the water. Various catalysts were described and characterized, and the catalytic activities in PMS oxidation system were investigated. Most important of all, the mechanism of different catalysts in the catalytic PMS solution was illustrated. The results showed that the incorporation of $CoFe_2O_4$ had the highest catalytic performance in PMS oxidation for DBP degradation. All catalysts presented favorable recycling and stability in the repeated batch experiment. The catalytic process showed a dependence on initial pH, and an uncharged surface of the catalyst was more profitable for sulfate radical generation. H_2-TPR and CVs analysis indicated that the sequence of the catalyst's reducibility in PMS solution was $CoFe_2O_4 > CuFe_2O_4 > MnFe_2O_4 > ZnFe_2O_4$, which had a close connection with the activity of metal ion in A site of the catalysts. The surface hydroxyl sites played an important role in the catalytic process, and its quantity determined the degradation of DBP. Moreover, the reactive species in PMS/MFe_2O_4 system were identified as sulfate radical and hydroxyl radical. The promotion of these radical's reaction was due to the fact that a balance action in the process of M^{2+}/M^{3+}, O^{2-}/O_2, occurred, and at the same time, PMS was catalyzed.

1. Introduction

Di-n-butyl phthalate (DBP) belongs to the family of phthalic acid esters (PAEs), a kind of refractory pollutant with high toxic and carcinogenic properties which is used primarily as plasticizers, adhesives, and printing inks [1,2]. It is relatively difficult to be removed from the water with traditional treatment processes. Advanced oxidation process (AOPs) is becoming a more and more efficient and important technology for water decontamination [3]. Catalytic ozonation with heterogeneous catalysts is an alternative to improve the degradation of recalcitrant pollutants by •OH without extra addition of chemicals and energy into the water [4]. Supported and unsupported metal oxides, such as CeO_2, TiO_2, MnO_2, Co_3O_4, V_2O_5, goethite, or transition metals deposited on several materials (alumina, activated carbon, and MCM-41, etc.) are the most frequently used ozonation catalysts having been studied [5,6]. However, the current catalysts are difficult to be separated from the water [7]. Furthermore, the removal efficiency and the stability of catalytic process need to be enhanced. This technology also suffers from drawbacks such as high cost in the production, and transports as well as poor selective for oxidation [8]. These problems have become the main limitations for the application of catalysts in the field of the water treatment.

During the past years, sulfate radical has attracted an increasing interest among researchers as an alternative to hydroxyl radical for the degradation of recalcitrant organic pollutants [9]. It has been found that $SO_4^{-\bullet}$ is more powerful and selective for oxidation than •OH in general [10,11]. Furthermore, PMS has a low energy input, and it is a cost-effective and environmental friendly oxidant [10]. Therefore, it is meaningful to find an effective way to produce more $SO_4^{-\bullet}$ in the oxidation system.

The $SO_4^{-\bullet}$ is mainly produced by metal ions such as Co^{2+}, Mn^{2+}, Fe^{2+}, Ru^{3+}, and Ag^{+} [12,13], etc., which can induce PMS or PDS. However, the reuse and the toxicity of the metal catalysts, as well

* Corresponding authors. Tel.: +86-451-82569890; fax: +86-451-86282292.
E-mail addresses: rym0606@163.com (Y. Ren), majun@163.com (J. Ma).

http://dx.doi.org/10.1016/j.apcatb.2014.10.051
0926-3373/

as the associated secondary contamination to the environment, also pose some challenges in such homogeneous processes. So, metals, metal oxides, and supported metal oxides as heterogeneous catalysts are employed [14–16]. But the metal leak cannot be completely avoided [17]. Therefore, it is desirable to develop a novel catalyst with good separation and remarkable catalysis to produce the active sulfate radicals in the water treatment. With the further search of heterogeneous catalyst, magnetic spinel-type ferrite particles with a general formula MFe_2O_4 (M = Mn, Fe, Co, Ni, and Cu, etc.) have been used in several applications. Recently, the spinel ferrites are being used by some to remove heavy metals from the water due to the abundant surface hydroxyl groups and magnetic property [18]. The photocatalytic and catalytic activities of the spinel ferrites have been reported. $ZnFe_2O_4$ exhibits notable photocatalytic activity for H_2O_2 under visible light irradiation [19]. Catalytic ozonation by $NiFe_2O_4$ is also reported to destruct DBP in our previous study [20]. Recently, $CuFe_2O_4$ and $CoFe_2O_4$ are found to be used as heterogeneous catalysts in PMS activation for oxidation of organic pollutants [21–23]. The difference of PMS activation may be related to the activity of metal ions in crystal phase of various spinel ferrites. However, up to now, the mechanism of PMS activated by various catalysts has not been further researched.

The purposes of this research are as follows: (i) to investigate the activity and stability of different MFe_2O_4 (M = Co, Cu, Mn, and Zn) for DBP degradation in the catalytic PMS oxidation solution, (ii) to explain the reason of DBP degradation by H_2-TPR and cyclic voltammetry in different catalytic PMS oxidation solution, (iii) to illustrate the reaction mechanism for PMS activation occurring on the catalysts surface by confocal Raman analysis, in situ FT-IR analysis, XPS analysis and other batch reaction experiments.

2. Experimental

2.1. Chemicals

Di-n-butyl phthalate (DBP), cobalt nitrate hexahydrate ($Co(NO_3)_2{\cdot}6H_2O$), copper nitrate trihydrate ($Cu(NO_3)_2{\cdot}3H_2O$), manganese nitrate solution 50% ($Mn(NO_3)_2{\cdot}50\%$), zinc nitrate hexahydrate ($Zn(NO_3)_2{\cdot}6H_2O$), iron nitrate nonahydrate ($Fe(NO_3)_3{\cdot}9H_2O$), tert-butyl alcohol (TBA), sodium dihydrogen phosphate (NaH_2PO_4), and methanol (Me) were of analytical grade and obtained from Tianjin Kermel Chemical Reagents Company (Tianjin, China). Potassium peroxymonosulfate (available as Oxone, PMS) was of ACS reagent grade and purchased from Sigma Aldrich. The fresh eggs were bought from the local market. The experimental solutions were prepared with deionized water.

2.2. Catalysts preparation and characterization

Magnetic spinel ferrites were prepared in a sol-gel process with egg white as previously reported [20]. The X-ray powder diffraction (XRD) was performed on a max-TTR-III diffractometer (Rigaku D, Japan). The magnetic property was measured at room temperature with a vibrating sample magnetometer (Lakeshore 7410, America). X-ray photoelectron spectroscopy (XPS) analysis was performed with K-Alpha (Thermofisher, America) using an Al Ka (1361 eV). All lines recorded were calibrated to the C 1s line at 284.6 eV. The measure of H_2-TPR, Cyclic voltammograms (CVs), and Raman spectra are shown in supporting information.

2.3. Catalytic degradation and reuse experiments

Experiments were completed in a 500 mL flask at 20 ± 2 °C. A certain amount of PMS and DBP were added into a final volume of 500 mL deionized water. 0.1 mol L^{-1} NaOH was used to adjust the solution pH. The oxidation reaction was started after adding the catalyst. Magnetic stirring was applied during the reaction at a rotary speed of 850 rpm at room temperature (20 ± 2 °C). Samples were withdrawn by a glass syringe and quenched by sodium nitrite before analysis, and then it was filtrated by a cellulose acetate membrane of 0.45 μm pore size for analysis. After each run, the catalyst was recovered under a magnetic field and washed with deionized water before drying at 80 °C for reuse. Two sets of quenching experiments were performed to determine the radical species forming in the MFe_2O_4/PMS system by using TBA and Me as the quenching agents, respectively. The used catalysts were subjected to centrifugal separation and dried for the recovery experiment. The reused experiments were carried out under the above reaction condition after compensation of the mass loss with virgin catalysts. In order to test the reproducibility, the experiments were carried out in triplicates and the error of reproducibility was added.

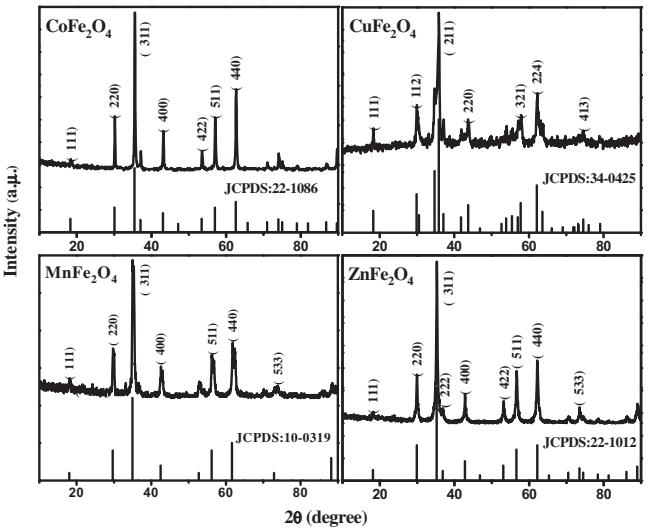

Fig. 1. XRD patterns of different catalysts.

2.4. Analysis

The concentration of DBP in the aqueous solution was analyzed by a high-performance liquid chromatograph (HPLC, Agilent 1200 Infinity, Germany) using an Atlantis dc18 column (4.6 mm × 150 mm). DBP were quantified at λ = 230 nm with water and methanol with ratio of 2:8 (v/v %) at a flow rate of 1.0 mL min^{-1}. Free metal ions were decided by an Inductively Coupled Plasma Optical Emission Spectrometer (ICP-OES, PerkinElmer, America). The pH_{zpc} of MFe_2O_4 was determined by mass titration and the pH value was measured by a pH meter (METTLER). The quantity of surface hydroxyl sites was measured by a saturated deprotonation method [24].

3. Results and discussion

3.1. Characterization of catalysts

XRD patterns of different MFe_2O_4 (M = Co, Cu, Mn, and Zn) are shown in Fig. 1. It can be seen that $CoFe_2O_4$ exhibits the typical pattern of spinel ferrite with seven well-defined peaks occurring at 2θ = 18.38°, 30.20°, 35.56°, 43.18°, 43.56°, 57.06°, and 62.68°. These peaks are corresponded to the Bragg planes of (1 1 1), (2 2 2), (3 1 1), (4 0 0), (4 2 2), (5 1 1), and (4 4 0), respectively. The major crystal phase of $CoFe_2O_4$ is in a good agreement with JCPDS: 22-1086. As for $CuFe_2O_4$, which is performed in space group I41/amd (141), the XRD pattern shows three intense diffraction peaks at 2θ angle of 30.00°, 35.88°, and 62.30°, respectively. These are well matched

Table 1
Some parameters of the MFe_2O_4 (M = Co, Cu, Mn, and Zn) samples.

Catalyst	Average crystallite size from XRD (nm)	Spinel lattice parameter (nm)	Ms (emu g^{-1})	Mr (emu g^{-1})	Surface hydroxyl groups (mmol g^{-1})
$CoFe_2O_4$	37.3	8.3742	58.9	33.55	0.5010
$CuFe_2O_4$	13.5	8.6408	24.9	10.80	0.4407
$MnFe_2O_4$	18.5	8.4567	46.2	4.24	0.4067
$ZnFe_2O_4$	43.5	8.4341	7.1	0.60	0.3645

with the published JCPDS: 34-0425 for the tetragonal $CuFe_2O_4$ spinel [25]. The diffraction peaks of $MnFe_2O_4$ and $ZnFe_2O_4$ match well with the spinel-type of JCPDS: 10-0319 and JCPDS: 22-1012, respectively, which are all performed in space group Fd – 3m (227) and belong to ferroxcube. The crystallite size and lattice parameters are summarized in Table 1. The average crystallite size of MFe_2O_4 is calculated from X-ray line broadening using Scherrer's equation (i.e. $D = 0.89\lambda/(\beta\cos\theta)$, where λ is the wavelength of the X-ray radiation, θ is the diffraction angle, and β is the full width at half maximum (FWHM) [26]. It is discovered that the average crystallite size of MFe_2O_4 ranges between 18 nm and 44 nm, and the lattice parameters are 8.3742–8.6408 nm, which demonstrates the changes of component and stress in the interior crystal. The structure of spinel ferrites is entirely detectable and indicates well crystallinity with different elements in A site. Furthermore, it is obviously seen that all the MFe_2O_4 are spinel and display the similar diffraction peak at the crystal face of (1 1 1), which can combine with hydroxyl groups easily in the water [27].

The magnetization characters of MFe_2O_4 at room temperature are shown in Fig. 2 and Table 1. The values of specific magnetization (Ms) are found to be 58.9, 24.9, 46.2, and 7.1 emu g^{-1} for $CoFe_2O_4$, $CuFe_2O_4$, $MnFe_2O_4$, and $ZnFe_2O_4$, respectively. Except for $ZnFe_2O_4$, all the ferrites possess a good magnetic property at room temperature and can be easily separated under the magnetic field, which is helpful in the recycling.

3.2. Activity and stability of catalysts

Other catalysts are used as a reference to evaluate the activity and stability of different catalysts in improving DBP degradation. Fig. 3 shows DBP degradation in PMS solution alone and PMS solution coupled with $ZnFe_2O_4$, $MnFe_2O_4$, $CuFe_2O_4$, $CoFe_2O_4$, and Co^{2+} and Fe^{3+}, respectively. As is shown that DBP is degraded quickly, and more than 81.0% of it is destructed within 30 min at PMS and $CoFe_2O_4$ doses of 0.02 mmol L^{-1} and 0.1 g L^{-1}, respectively, while nearly no DBP removal is seen for PMS alone oxidation. $CoFe_2O_4$ exerts little DBP adsorption with less than 15.0% adsorbed onto the surface, which confirms DBP degradation in the different PMS/MFe_2O_4 oxidation system. 62.3%, 42.3%, and 30.0% of DBP are degraded within 30 min at PMS/$CuFe_2O_4$, PMS/$MnFe_2O_4$, and PMS/$ZnFe_2O_4$ couples, respectively. $CoFe_2O_4$ presents the highest catalytic effect on DBP degradation. It suggests that Co and Fe ions have the best synergistic effect on DBP degradation in the PMS solution. Free metal ions can activate PMS to produce •OH and/or $SO_4^{-\bullet}$, resulting in the removal of organic pollutants [28]. The DBP removal rate is studied in homogeneous PMS catalytic reaction. Under the same reaction condition, the leaking concentrations of Co ions (518 μg L^{-1}) and Fe ions (28 μg L^{-1}) show very low activity with less than 5% of DBP removal within 30 min. Obviously, DBP degradation in PMS/MFe_2O_4 solution follows a heterogeneous catalytic reaction, which is attributed to the synergistic effect of PMS and MFe_2O_4.

The concentrations of released metal ions from the catalysts after 30 min reaction are shown in Fig. S1(a). It is found out that the concentrations of various metal ions are all very low in the PMS oxidation solution. The highest concentration of released Co and Cu ions can reach 518 μg L^{-1}, accounting for 0.05% to the total ferrites weight. However, the concentrations of released Mn and Zn ions are 105 and 126 μg L^{-1} in the solution, respectively. Evidently, the average concentration of Fe ions leakage is about 28 μg L^{-1}, occupying 0.03% of the total ferrites weight. They are below the discharge limit regulated by Chinese Environmental Protection Agency and US EPA. The catalysts are stable in the PMS oxidation solution.

The four catalysts are recovered and reused for seven times with the same initial batch of oxide catalysts. As shown in Fig. S1 (b), under the same reaction condition, the removal of DBP in various PMS/MFe_2O_4 oxidation system keeps almost constant and is only decreased at the range of 2–3% after seven recycle times. They show excellent stability for DBP degradation during catalyzing PMS oxidation. This might be related to the high stability of the spinels structure. Zhang et al. also observed that $CuFe_2O_4$ still had high activity in iopromide degradation after having used seven times in PMS oxidation, which was ascribed to its good crystallization [21]. With the excellent stability and magnetic property, MFe_2O_4 with different A site (the site of M with different metal ions) is suitable for pollutants degradation in PMS catalytic system.

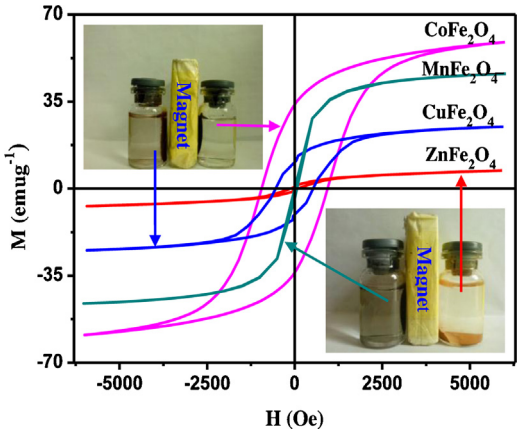

Fig. 2. Magnetic hysteresis loops of different catalysts.

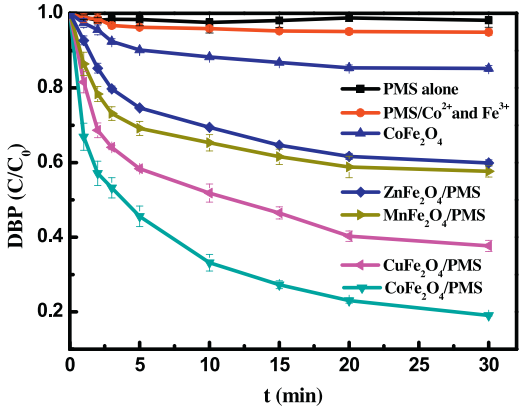

Fig. 3. DBP degradation in different PMS oxidation systems. [PMS] = 20 μmol L^{-1}, [catalyst] = 0.1 g L^{-1}, $[DBP]_0$ = 2 μmol L^{-1}, $[Co^{2+}]$ = 0.518 mg L^{-1}, $[Fe^{3+}]$ = 0.028 mg L^{-1}, pH = 7.0.

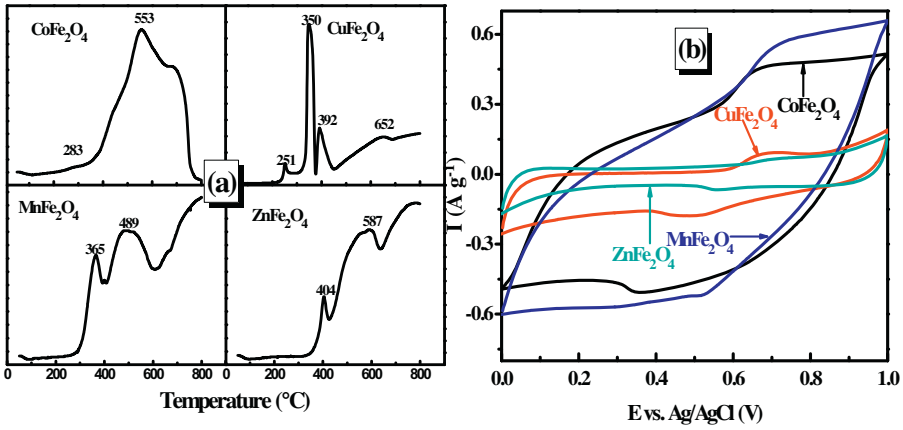

Fig. 4. (a) H_2–TPR profiles of different catalysts and (b) cyclic voltammograms (CVs) obtained on different MFe_2O_4 electrode in a solution of 0.1 M Na_2SO_4 and peroxymonosulfate after 8th cycle. Scan rate = 50 mV s^{-1}, pH = 7.0.

3.3. Isothermal H_2 reduction and electrochemical property of catalysts

According to our DBP degradation experiment in PMS oxidation system, it has been confirmed that catalysts with different A site reveal distinct catalytic redox performance. To illustrate this phenomenon, it is important to study the H_2 reduction and electrochemical property of different ferrites. Fig. 4(a) shows the H_2-TPR profiles of the four catalysts. Clearly, the four ferrites exhibit different TPR profiles with the temperature increasing from 0 °C to 800 °C. It can be found that $CoFe_2O_4$, $MnFe_2O_4$, and $ZnFe_2O_4$ have yielded two peaks, while $CuFe_2O_4$ produces three peaks under the same temperature range. Concretely, $CoFe_2O_4$ shows two shoulder peaks at about 283 °C and 553 °C. According to the report [29], $CoFe_2O_4$ begins to be reduced at about 256 °C, which deduces the production of Fe_3O_4 and metal Co. Furthermore, the generated Co in the process can promote the reduction of ferrite. It is easy to observe the peak at the temperature of 283 °C owing to the capacity of adsorption for metal Co and dissociation for hydrogen. With the increase of temperature, $CoFe_2O_4$ is further reduced to metal Co and Fe_3O_4. Fe_3O_4 is further reduced to α-Fe at the higher temperature [30]. It can be seen that $CuFe_2O_4$ sample exhibits three distinct peaks. The peaks appearing at the temperature range of 240–400 °C are ascribed to the reduction of $CuFe_2O_4$ to metallic Cu and Fe_2O_3, and then to the subsequent reduction of Fe_2O_3 to Fe_3O_4. Fe_3O_4 is fully reduced to Fe after the high temperature reduction at 450–600 °C. Obviously, it is hard to define a clear boundary between each of the reduction steps. As for $MnFe_2O_4$ and $ZnFe_2O_4$, the peaks at the temperature range of 300–450 °C belong to the reduction of ferrites to metallic Mn/Zn and Fe_2O_3. After the higher reduction temperature at 450–600 °C, Fe_3O_4 is fully reduced to Fe. Obviously, the initial reduction peaks of the four ferrites appear at the temperature of 283 °C, 350 °C, 365 °C, and 404 °C for $CoFe_2O_4$, $CuFe_2O_4$, $MnFe_2O_4$, and $ZnFe_2O_4$, respectively. The sequence of reductibility for the catalysts in the PMS oxidation solution is $CoFe_2O_4 > CuFe_2O_4 > MnFe_2O_4 > ZnFe_2O_4$. This suggests that $CoFe_2O_4$ has the lowest reduced temperature resulting in excellent reduction activity among the four catalysts. Importantly, the reduced products of metal Co and Fe exert a great effect on improving the reductibility of $CoFe_2O_4$, and the interaction of the PMS and $CoFe_2O_4$ has a high catalytic effect on the DBP degradation.

In order to observe the electron transfer process at water–catalyst interface and compare the redox capacity of different catalysts, the cyclic voltammetry behaviors of various MFe_2O_4 on electrodes are investigated in a mixed solution of 0.1 mol L^{-1} Na_2SO_4 and peroxymonosulfate oxidate. Fig. 4(b) has shown consecutive CV scan after eight cycles and all samples have exhibited identical curves in the shape. $CoFe_2O_4$ electrode gives a well-defined reduction potential peak at 0.357 V, which is possibly contributed to the cycle of Co(I)/Co(III). At the peak of 0.483 V, a gentle redox couple is assignable to the redox of Cu(II)/Cu(III) species. Likewise, a similar redox couple appears at 0.513 V owing to the reaction of Mn(II) in the mixed PMS solution. Meanwhile, $ZnFe_2O_4$ electrode shows an indistinct redox peak at 0.559 V, which may be related to the activity of the reduction of Zn in the mixed solution. It is obvious that a pair of cathodic and anodic peaks in the CV curves can be clearly found, which indicates the fast redox reaction of $CoFe_2O_4$ and $CuFe_2O_4$ in PMS oxidation solution [31]. $CoFe_2O_4$ electrode displays a couple of redox peaks with the reduction potential separation (ΔE_P) of 0.418 V. A decrease of the ΔE_P of $CuFe_2O_4$, $MnFe_2O_4$, and $ZnFe_2O_4$ electrode are obtained as 0.241 V, 0.228 V, and 0.222 V in the CV curve, respectively. This may be contributed to a low electron transfer rate and the activity of various catalysts. In order to eliminate the interference of impossible peak in the solution, the cyclic voltammetry curves of the carrier in Na_2SO_4 or PMS solution are studied and shown in Fig. S2. There is no effect on the peaks appearance for Na_2SO_4 and PMS in the oxidation reaction system. It is worth noting that the reduction potential is consistently diverse with different A site element of MFe_2O_4, and the sequence of deoxidize potential in the PMS oxidation solution reduction capacity is $CoFe_2O_4 > CuFe_2O_4 > MnFe_2O_4 > ZnFe_2O_4$. The capacity of reduction potential may be related to the chemical activity and the capacity of transitive electron of metal ions in the process of the reduction and oxidation.

3.4. Effect of surface hydroxyl site and pH on catalytic activity of MFe_2O_4

Guan et al. have found that the surface OH has an important effect on $CuFe_2O_4$ catalysis PMS [28]. It is reported that the reduction of COD depends strongly on the concentration of surface OH during the TiO_2 catalytic ozonation of phenol [32]. In addition, Tamura et al. have presented a method as to how to measure the quantity of surface hydroxyl site [24]. Therefore, the quantity of surface hydroxyl sites for different A site catalysts are measured in this experiment. The relationships between the quantity of surface hydroxyl sites, first-order rate constant and initial degradation rate have been set up. The results are shown in Table 1 and Fig. 5. Obviously, different surface OH site concentration can be observed

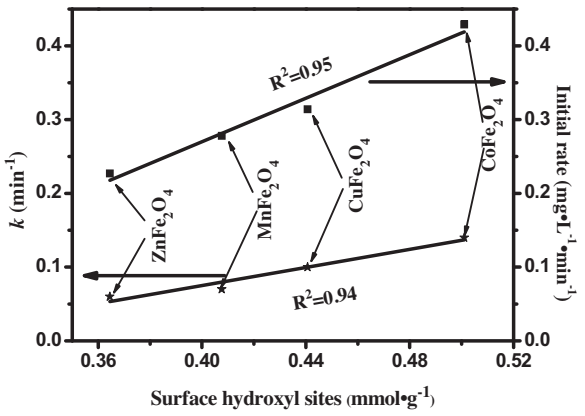

Fig. 5. Relationship between simulated rate constant, initial rate, and surface hydroxyl sites in different PMS oxidation systems.

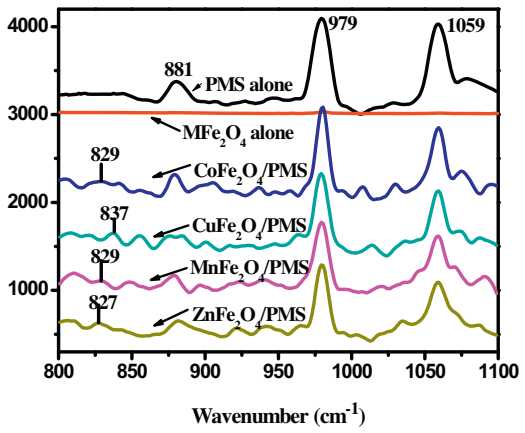

Fig. 6. Raman spectra in different PMS oxidation systems. pH = 7.0.

on the four catalysts. The hydroxyl sites on $CoFe_2O_4$ surface have the highest quantity of 0.5010 mmol g^{-1}, and the others are 0.4407, 0.4067, and 0.3654 mmol g^{-1} on the surface of $CuFe_2O_4$, $MnFe_2O_4$, and $ZnFe_2O_4$, respectively. Fig. 5 shows that there is a good linear correlation (R^2 = 0.95) between initial DBP degradation rate and the quantity of surface OH sites in different PMS oxidation systems, and also a fine linear relationship (R^2 = 0.94) is found between the reaction rate (k) and the quantity of surface OH sites. It indicates that DBP degradation depends greatly on the quantity of surface OH sites. It is reported that the quantity of surface OH sites depends on the amount of oxygen vacancy sites [33,34]. The four catalysts prepared in our experiment have the same morphology and crystal phase. Moreover, our results show that the element of A site is responsible for catalytic PMS, and Co is the most appropriate element for the system. It can be concluded that the quantity of surface hydroxyl sites has a relationship with binding sites on the surface of catalysts. The more surface hydroxyl sites occupy the binding sites on the surface of catalysts, the easier the oxidation reactions occur.

The influence of initial pH ranging from 5.0 to 9.0 on DBP degradation is studied in the process of PMS oxidation. The existing form of PMS depends mainly on solution pH and the second pK_a. The pK_a of PMS (second pK_a of its parent acid) is 9.4 and its parent acid (H_2SO_5) is a strong acid as sulfuric acid [35,36]. Thus, in the pH range of 5.0–9.0 investigated, HSO_5^- is the only PMS species appearing in the solution at acid and neutral pH values. pH_{zpc} is measured by adding the powders and shown in Fig. S3.

DBP degradation has the same change with different pH values increasing, and it reaches the maximum when the pH value closing to pH_{zpc} during catalytic PMS. pH will determine the charge property of surface hydroxyl groups at oxide/water interface. Take $CoFe_2O_4$/PMS as an example. It is obvious that $CoFe_2O_4$ catalytic PMS substantially enhances the DBP degradation from 46% to 71% at pH 5.0–7.0. At pH < 7.7 (pH_{zpc}), the surface of $CoFe_2O_4$ becomes protonated and positively charged. More HSO_5^- is absorbed onto $CoFe_2O_4$ surface and this will promote the form of $SO_4^{-\bullet}$ and •OH. Moreover, the increasing liberative OH^- ions in the solution can also accelerate PMS decomposition to form active species which react with the organics in a non-selective mode with a higher reaction rate constant. However, the surface gets deprotonated at 7.0 < pH < 9.0, and it is difficult for the combination of HSO_5^- onto $CoFe_2O_4$ surface. Although the continuous increasing of OH^- ions may accelerate PMS decomposition, the DBP removal decreases from 71% to 37%. This indicates that the combination of HSO_5^- onto the surface of $CoFe_2O_4$ is most important during the catalytic PMS process.

3.5. Possible active radical and sites

PMS can generate •OH and/or $SO_4^{-\bullet}$ by homogeneous or heterogeneous activations [13,23]. As we know, methanol (Me) is widely used as a scavenger of hydroxyl and sulfate radicals, while tert-butyl alcohol (TBA) is an effective quenching agent for hydroxyl radicals. Me reacts with •OH and $SO_4^{-\bullet}$ to form hydroxylmethyl radical ($\bullet CH_2OH$), which may stimulate the decomposition of PMS into radicals [9]. Inhibition of TBA and Me on DBP degradation in PMS/$CoFe_2O_4$ oxidation system can be seen in Fig. S4. DBP degradation rate was reduced with the increasing of TBA and Me dosages. At low (10 mmol L^{-1}) or high concentration (300 mmol L^{-1}), Me inhibits DBP degradation more significantly than TBA. Nearly no DBP removal is seen at Me dosage of 300 mmol L^{-1}. The difference of inhibition by TBA and Me on DBP degradation is due to the formation of $SO_4^{-\bullet}$. The results suggest that the main radical types generated during the activation of PMS by MFe_2O_4 are $SO_4^{-\bullet}$ and •OH. Further experiments have been conducted to identify the reactive species in MFe_2O_4/PMS system.

Characterization of the catalysts surface are conducted with confocal Raman and ATR-FTIR during catalytic decomposition of PMS. Raman (Fig. 6) indicates that the intensity of the peaks at 881 cm^{-1} and 1059 cm^{-1} are due to SO_5^{2-}, and a sharp peak at around 979 cm^{-1} is ascribed to SO_4^{2-} for PMS alone. However, no peaks are produced for the ferrites alone. Meanwhile, new broad peaks appear at about 827-837 cm^{-1} during different catalytic decomposition of PMS. These peaks can be attributed to the formation of a peroxo species bond to surface metal sites, which will finally detach from the surface as O_2 [37–39]. This explanation is supported by the research of Zhang et al. [21].

Fig. S5 indicates ATR–FTIR spectra of various MFe_2O_4 surface in the presence and absence of PMS. The peaks at the region of 900–1340 cm^{-1} for PMS alone are generally assigned to the symmetric and asymmetric stretching of the S—O bonds of either HSO_5^- or SO_4^{2-} [40]. However, about blue-shift of 10 cm^{-1} at the peak of 1200 cm^{-1} is observed when different MFe_2O_4 is added into PMS solution, which indicates the change of S—O bond. Such characterization demonstrates that $SO_4^{-\bullet}$ could be produced from PMS oxidation. Peroxomonosulfate radical ($SO_5^{-\bullet}$) might also be formed, but it would not contribute to DBP degradation for its lower redox potential [41]. Phosphate is used to investigate the role of surface hydroxyl groups in catalytic PMS due to its strong bonding with the active sites on the catalyst surface (Fig. S4). The increment of phosphate concentration significantly inhibits DBP degradation in the catalytic PMS system. The phosphate has more affinity with the active site than the surface hydroxyl groups, and it will replace the hydroxyl groups on the surface of $CoFe_2O_4$, which

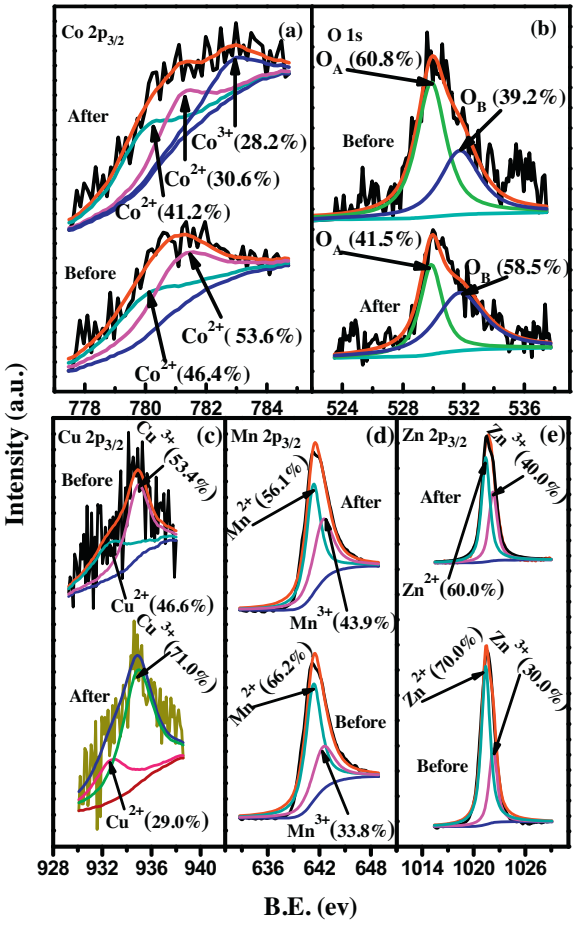

Fig. 7. XPS spectra of different catalysts before and after the reaction with PMS. pH = 7.0.

suppresses the decomposition of PMS to produce sulfate radical [42]. The results verify that the surface hydroxyl groups will be the major factor responsible for the activation of PMS, and the mechanism of catalytic PMS on the surface of MFe_2O_4 is proposed based on this experiment.

3.6. Activation mechanism of PMS

Fig. 7 presents the XPS of M 2p (Co, Cu, Mn, and Zn) and O 1s XP spectra of the catalysts before and after oxidation process. The characteristic satellites of Fe2p confirm that no redox reaction has occurred for iron ion on the surface of the catalysts after the reaction (data are not shown). Only the metals in the A site have the valent change. Fig. 7a shows that before catalytic oxidation process, Co $2p_{3/2}$ peak of $CoFe_2O_4$ [43] are measured, and two peaks with binding energy appearing at 779.90 and 781.15 eV are ascribed to Co^{2+} ions in octahedral and tetrahedral sites, respectively. The relative contributions to the overall Co intensity are of 46.4% and 53.6%, respectively. However, the Co $2p_{3/2}$ peak after catalytic oxidation process is composed of three peaks at 779.90, 781.15 and 782.80 eV, with relative contributions to the overall Co intensity of 41.2%, 30.6% and 28.2%, respectively, which is ascribed to Co^{2+} in octahedral sites, tetrahedral sites and Co^{3+} in octahedral sites [43]. Co is mainly present in +2 valent states before reaction and undergoes a partial increase to +3 valent states after catalytic reaction. This could be due to the coexisting oxidation and reduction conditions in the solution. The oxidizing reaction occurs on the surface and Co^{2+} would provide the electrons, in order to keep the balance of charge on the catalyst surface, Co^{2+} will accept the electrons from

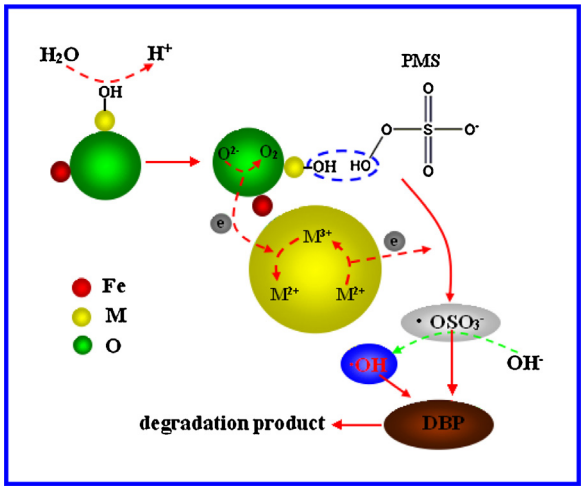

Fig. 8. Activation mechanism of MFe_2O_4 inducing PMS.

the system. It manifests the involvement of Co^{2+}–Co^{3+}–Co^{2+} redox processes during the reaction.

The high-resolution O 1s spectra of $CoFe_2O_4$ before and after oxidation are resolved into two individual peaks located at 529.87 and 531.76 eV (Fig. 7b), which are assigned to the surface lattice oxygen of metal oxides (O^{2-}, denoted as O_A) and adsorbed oxygen or surface hydroxyl species (denoted as O_B) [44]. Some researchers report that O^{2-} and surface hydroxyl groups are active oxygen species, and that they play a critical role in oxidation reaction [45]. After catalytic reaction, it is found out that the area ratios of both peaks change in a massive way, that is, the relative contents of lattice oxygen reduce from 60.8% to 41.5%, and the relative contents of adsorbed oxygen increase from 39.2% to 58.5%, indicating that both of them are involved in the catalytic reaction. The increase of adsorbed oxygen concentration might be ascribed to the formation of M—OH groups (M: Co or Fe) or O_2 adsorbed on the catalyst surface. The decrease of lattice oxygen in $CoFe_2O_4$ may be oxidized by Co^{3+} with its reduction to Co^{2+}. Polnišer has concluded that Cu^{2+} would oxidize the lattice oxygen to O_2, and Cu^{2+} is simultaneously reduced to Cu^{+} during the selective oxidation of methan over copper iron pyrophosphate catalysts [46]. Similar conclusions are drawn from XPS spectra (Fig. 7c–e) of other catalysts ($CuFe_2O_4$, $MnFe_2O_4$, and $ZnFe_2O_4$) before and after catalytic PMS oxidation process. Cu, Mn, or Zn is present in +2 and +3 valent states in the catalyst before, and the percentage of all of them are changed after the reaction. It shows that the reaction of M^{2+}–M^{3+}–M^{2+} is involved during the PMS oxidation.

Surface hydroxyl site has been proved to be an important active site for DBP degradation in the above experiment. FTIR and XPS results indicate the production of oxide groups with sulfur compound, and the transformation of the existence state for different metal ions (Co, Cu, Mn, and Zn) and oxygen on MFe_2O_4 surface. The activation mechanism of MFe_2O_4 inducing PMS is presented in Fig. 8 and the reaction process is shown in Eqs. (1)–(4). It is assumed that metal ions act as Lewis sites and combine with H_2O resulting in lots of hydroxyls forming activated oxygen species on the surface of MFe_2O_4. Meanwhile, HSO_5^- is bonded in the form of MFe_2O_4—O—H—HSO_5^- through hydrogen bond in the solution. Firstly, metal ions in A site of catalysts serve as active sites to transfer redox electrons with the oxidation of M^{2+} to M^{3+}. During this process, the electrons are discharged and the H—O and O—O bond will be cracked after accepting the electrons, and the intermediate is supposed to be $SO_4^{-\bullet}$, •OH and OH^- in the solution as described in Eqs. (1) and(2). A typical chain reaction for the production of $SO_4^{-\bullet}$ and •OH will interact with DBP leading to its degradation.

Secondly, in order to keep the balance of the charge on MFe_2O_4 surface, the lattice oxygen is oxidized to O_2 by the donated electrons out flowing in the process of simultaneous reduction from M^{3+} to M^{2+} (Eqs. (3) and (4)). Meanwhile, O_2 in the solution will supply the oxygen-deficient bulk on the MFe_2O_4 surface to ensure the activity of catalysts. It is suggested that the balance among M^{2+}/M^{3+}, O^{2-}/O_2, and PMS catalyzed in the water is the main factor to keep the high catalytic performance.

$$\equiv M^{2+} + HSO_5^- \rightarrow \equiv M^{3+} + SO_4^{-\bullet} + OH^- \quad (1)$$

$$SO_4^{-\bullet} + OH^- \rightarrow SO_4^{2-} + \cdot OH \quad (2)$$

$$\equiv M^{3+} + HSO_5^- \rightarrow \equiv M^{2+} + SO_5^{-\bullet} + H_2O \quad (3)$$

$$SO_5^{-\bullet} + O^{2-} \rightarrow SO_4^{-\bullet} + O_2 \quad (4)$$

4. Conclusions

Magnetic ferrospinel MFe_2O_4 (M = Co, Cu, Mn, and Zn) was used as heterogeneous catalysts for PMS oxidation. It is found out that $CoFe_2O_4$ poses the highest catalytic activity towards PMS for the degradation of DBP among the four catalytic oxidation systems. MFe_2O_4 is stable in the PMS oxidation solution and can be reused seven times with high PMS catalytic effect. The sequence of catalytic effect for the DBP degradation in the PMS oxidation solution is $CoFe_2O_4 > CuFe_2O_4 > MnFe_2O_4 > ZnFe_2O_4$. The catalytic process is pH dependent and the surface hydroxyl sites are the main active sites for MFe_2O_4 in the catalytic PMS process. Furthermore, $SO_4^{-\bullet}$ and $\bullet OH$ are the main radicals to degrade DBP. The activities of A site metals in the catalysts have an important role in the PMS catalytic solution for DBP degradation. Also, the high catalytic activity can be attributed to the involvement reaction for M^{2+}/M^{3+} and O^{2-}/O_2, and PMS is catalyzed simultaneously in MFe_2O_4 catalytic process. The activation of PMS by spinel ferrites as green oxidation process has promising potentials in the application of contamination control.

Acknowledgments

We appreciate the financial support of the National Natural Science Foundation of China (Nos. 51378141, 51178134, 51108111, 21301038 and 21203040), Fundamental Research Funds for the Central Universities (no. HEUCF 201403009), Heilongjiang Natural Science Foundation (no. E201125) and Heilongjiang Education Office Foundation (no. 12513044).

Appendix A. Supplementary data

Supplementary data associated with this article can be found, in the online version, at http://dx.doi.org/10.1016/j.apcatb.2014.10.051.

References

[1] K. Fent, A.A. Weston, D. Caminada, Aquat. Toxicol. 76 (2006) 122–159.
[2] X.X. Hu, W. Shi, F.X. Zhang, F. Cao, G.J. Hu, Y.Q. Hao, S. Wei, X.R. Wang, H.X. Yu, Environ. Pollut. 173 (2013) 210–215.
[3] Z. Yang, H. Wang, M. Chen, M. Luo, D. Xia, A. Xu, Q. Zeng, Ind. Eng. Chem. Res. 51 (2012) 11104–11111.
[4] G. Balasubramanian, D.D. Dionysiou, M.T. Suidan, I. Baudin, Appl. Catal. B: Environ. 47 (2004) 73–84.
[5] E.C. Chetty, V.B. Dasireddy, S. Maddila, S.B. Jonnalagadda, Appl. Catal. B: Environ. 117–118 (2012) 18–28.
[6] R.H. Huang, B.Y. Lan, Z.Y. Chen, H.H. Yan, Q.Y. Zhang, Chem. Eng. J. 180 (2012) 19–24.
[7] Y.M. Dong, H.X. Yang, K. He, S.Q. Song, A.M. Zhang, Appl. Catal. B: Environ. 85 (2009) 155–161.
[8] S. Yuan, Y. Fan, Y. Zhang, M. Tong, P. Liao, Environ. Sci. Technol. 45 (2011) 8514–8520.
[9] Y.H. Guan, J. Ma, X. Li, J. Fang, L. Chen, Environ. Sci. Technol. 45 (2011) 9308–9314.
[10] P.R. Shukla, S. Wang, H. Sun, H.M. Ang, M. Tadé, Appl. Catal. 100 (2010) 529–534.
[11] G. Lente, J. Kalmár, Z. Baranyai, A. Kun, I. Kék, D. Bajusz, M. Takács, L. Veres, I. Fábián, Inorg. Chem. 48 (2009) 1763–1773.
[12] G.P. Anipsitakis, D.D. Dionysiou, Environ. Sci. Technol. 38 (2004) 3705–3712.
[13] G.P. Anipsitakis, D.D. Dionysiou, M.A. Gonzalez, Environ. Sci. Technol. 40 (2006) 1000–1007.
[14] E. Saputra, S. Muhammad, H.Q. Sun, H.M. Ang, M.O. Tade, S.B. Wang, Environ. Sci. Technol. 47 (2013) 5882–5887.
[15] E. Saputra, S. Muhammad, H.Q. Sun, H.M. Ang, M.O. Tade, S.B. Wang, Appl. Catal. B: Environ. 142 (2013) 729–735.
[16] W. Zhang, H.L. Tay, S.S. Lim, Y.S. Wang, Z.Y. Zhong, R. Xu, Appl. Catal. B 95 (2010) 93–99.
[17] H.Q. Sun, H.W. Liang, G.L. Zhou, S.B. Wang, J. Colloid Interface Sci. 394 (2013) 394–400.
[18] W. Tang, Y. Su, Q. Li, S. Gao, J.K. Shang, Water Res. 47 (2013) 3624–3634.
[19] M.H. Su, C. He, V.K. Sharma, M. Abou Asi, D. Xia, X.Z. Li, H.Q. Deng, Y. Xiong, J. Hazard. Mater. 211 (2012) 95–103.
[20] Y.M. Ren, Q. Dong, J. Feng, J. Ma, Q. Wen, M.L. Zhang, J. Colloid Interface Sci. 382 (2012) 90–96.
[21] T. Zhang, H. Zhu, J.-P. Croué, Environ. Sci. Technol. 47 (2013) 2784–2791.
[22] Y.B. Ding, L. Zhu, N. Wang, H. Tang, Appl. Catal. B: Environ. 129 (2013) 153–162.
[23] Q. Yang, H. Choi, S.R. Al-Abed, D.D. Dionysiou, Appl. Catal. B: Environ. 88 (2009) 462–469.
[24] H. Tamura, A. Tanaka, K-y. Mita, R. Furuichi, J. Colloid Interface Sci. 209 (1999) 225–231.
[25] P. Laokul, V. Amornkitbamrung, S. Seraphin, S. Maensiri, Curr. Appl. Phys. 11 (2011) 101–108.
[26] B.D. Cullity, S.R. Stock, Elements of X-ray Diffraction, 3rd ed, Prentice Hall, New Jersey, 2001.
[27] Y. Joseph, W. Ranke, W. Weiss, J. Phys. Chem. B 104 (2000) 3224–3236.
[28] Y.H. Guan, J. Ma, Y.M. Ren, Y.L. Liu, J.Y. Xiao, L.Q. Lin, C. Zhang, Water Res. 47 (2013) 5431–5438.
[29] L.J. Ma, R. Wu, H.D. Liu, W.J. Xu, L.S. Chen, Solid State Sci. 13 (2011) 2172–2176.
[30] L.J. Ma, L.S. Chen, S.Y. Chen, Mater. Chem. Phys. 114 (2009) 692–696.
[31] A.H. Lv, C. Hu, Y.L. Nie, J.H. Qu, Appl. Catal. B: Environ. 100 (1) (2010) 62–67.
[32] S. Song, Z.W. Liu, Z.Q. He, A.L. Zhang, J.M. Chen, Environ. Sci. Technol. 44 (2010) 3913–3918.
[33] A.A. Bonapasta, F. Filippone, G. Mattioli, P. Alippi, Catal. Today 144 (2009) 177–182.
[34] Y. Namai, O. Matsuoka, J. Phys. Chem. B 109 (2005) 23948–23954.
[35] S.K. Rani, D. Easwaramoorthy, I.M. Bilal, M. Palanichamy, Appl. Catal. A: Gen. 369 (2009) 1–7.
[36] G.A. Lawrance, C.B. Ward, Transition Met. Chem. 10 (1985) 258–261.
[37] V.V. Pushkarev, V.I. Kovalchuk, J.L. Itri, J. Phys. Chem. B 108 (2004) 5341–5348.
[38] K. Shimizu, Y. Murata, A. Satsuma, J. Phys. Chem. C 111 (2007) 19043–19051.
[39] T. Zhang, W. Li, W. Croue, Environ. Sci. Technol. 45 (2011) 9339–9346.
[40] J. Gonzalez, M. Torrent-Sucarrat, J.M. Anglada, Phys. Chem. Chem. Phys. 12 (2010) 2116–2125.
[41] P. Neta, R.E. Huie, A.B. Ross, J. Phys. Chem. Ref. Data 17 (1988) 1027–1284.
[42] R. Rosal, A. Rodríguez, M.S. Gonzalo, E. García-Calvo, Appl. Catal. B: Environ. 84 (2008) 48–57.
[43] Z. Zhou, Y. Zhang, Z. Wang, Appl. Surf. Sci. 254 (2008) 6972–6975.
[44] I.M. Ismail, B. Abdallah, M. Abou-Kharroub, O. Mrad, Nucl. Instrum. Methods B 271 (2012) 102–106.
[45] A. Galtayries, R. Sporken, J. Riga, G. Blanchard, R. Caudano, J. Electron. Spectrosc. Relat. Phenom. 88–91 (1998) 951–956.
[46] R. Polnišer, M. Štolcová, M. Hronec, M. Mikula, Appl. Catal. A: Gen. 400 (2011) 122–130.